ORIGINAL PAPER

Mesoporous amorphous MnO$_2$ as electrode material for supercapacitor

Mao-Wen Xu · Dan-Dan Zhao · Shu-Juan Bao · Hu-Lin Li

Abstract A kind of novel mesoporous, electrochemical active material, amorphous MnO$_2$ has been synthesized by an improved reduction reaction and using supramolecular as template. The synthesized sample was characterized physically by thermogravimetric analysis, X-ray diffraction, transmission electron microscope (TEM), and Brunauer–Emmett–Teller (BET) surface area measurement, respectively. Electrochemical characterization was performed using cyclic voltammetry and chronopotentiometry in 2 mol/l KOH aqueous solution electrolyte. The results of BET and TEM analysis indicated that supramolecular template plays an important role in the process of big specific surface area mesoporous material forming. After sintering at 200 °C, the sample still remained an amorphous structure, and its specific capacitance reached 298.7 F/g and presented a very stable capacitance after 500 cycles. In addition, the electrochemical process, such as ion transfer and electrical condition, was also investigated with electrochemical impedance spectroscopy.

Keywords Electrochemical capacitors (ECs) · MnO$_2$ · Mesoporous · Amorphous

Introduction

Transition metal oxides, such as porous NiO$_x$ [1], CoO$_x$ [2], and MnO$_2$ [3, 4], are promising candidates applicable in supercapacitors. Among these candidates, MnO$_2$ has been considered to be the most attractive alternative in terms of cheaper, more abundant, and more environmentally friendly than noble metal oxides and other transition metal oxide systems [5].

MnO$_2$ with different physical and chemical properties, such as crystallinity, amount of combined water, specific surface areas, and electrochemical performance, can be yielded under different synthesis conditions. Up to now, many routes for the preparation of MnO$_2$ have been developed including thermal oxidation of Mn(II) nitrates [6], chemical coprecipitation route [7], electrolysis of Mn (II) salts [8], and sol–gel method [5]. Among these methods, sol–gel process and electrochemical route have been considered as comparatively better methods for fabricating MnO$_2$ electrodes of ECs, which exhibit relative large specific capacitance, ranging from 110 to 220 F/g (from a single electrode) with excellent cycle life. But these preparation processes are very complicated and difficult to control [5, 9].

More recently, the discovery of M41S materials by the supramolecular templating mechanism ushered in a new era in synthesis chemistry [9, 10]. These mesoporous materials exhibit a high surface area, narrow pore size distribution, large pore volume, and high thermal stability, which allow them to be applied as catalysts, molecular sieves, host materials, and battery materials. Therefore, in this work, MnO$_2$ was prepared by using supramolecular as template. In the reaction process, the colloid MnO$_2$ precursor obtained is favorable to generate the mesoporous amorphous MnO$_2$. The unique mesopore system and large surface area are expected to favor ion transfer in the pore system and increase the MnO$_2$–electrolyte interfacial area, respectively. The main physiochemical properties and electrochemical performance of MnO$_2$ as electrode materials in 2 mol/l KOH electrolyte solution were analyzed. The

M.-W. Xu · D.-D. Zhao · S.-J. Bao · H.-L. Li (✉)
College of Chemistry and Chemical Engineering,
Lanzhou University,
Lanzhou 730000, People's Republic of China
e-mail: lihl@lzu.edu.cn

effect of calcination temperature on capacitance was also discussed. The results indicate that the obtained amorphous MnO_2 showed good performance as a supercapacitor.

Experimental

Materials preparation

All chemicals were of analytical grade and were used without further purification. MnO_2 was prepared by an improved reduction method and using supramolecular as template. The detailed process was as follows: Polyacrylamide (PAM) and polyvinyl alcohol (PVA) were dissolved in distilled water; a certain amount of ethanol was added subsequently. The obtained solution was heated and kept at 50 °C, and then the potassium permanganate aqueous solution was added slowly with magnetic stirring. After stirring for 1.5 h, a brown colloid was formed, and then it was washed several times with distilled water to remove any soluble products and dried at room temperature in air. The final step was to calcine the prepared precursor at different temperatures from 100 to 400 °C for 1.5 h. In addition, manganese oxide was also prepared following the same procedure without using supramolecular as template for comparison.

Characterization of structure and morphology

Thermogravimetric and differential thermal analysis (TG–DTA) was performed on Setarm TGDTA92A with α-Al_2O_3 as the reference substance at a heating rate of 10 °C/min. Structures of the products were characterized by X-ray diffraction (XRD), and XRD data were collected using a Rigaku D/MAX 2400 diffractometer with Cu Kα radiation (λ=0.15418 nm). Transmission electron microscope (TEM; Hitachi 600, Japan) was used to observe the morphology of the product. Nitrogen adsorption and desorption experiments were carried out at 77.3 K by means of a Nova 1200 (Quantachrome) analyzer. The surface area was calculated using the Brunauer–Emmett–Teller (BET) equation. Pore size distributions were calculated by the Barrett–Joyner–Halenda method using the desorption branch of the isotherm.

Electrode preparation and electrochemical characterization

The working electrodes of electrochemical capacitors were formed by mixing the prepared powder with 25 wt% acetylene black and 5 wt% polytetrafluorine-ethylene binder of the total electrode mass. A small amount of distilled water was then added to those mixtures to make them more homogeneous. The mixtures were pressed onto nickel foam current collectors (1.0×1.0 cm^2) to fabricate electrodes. All electrochemical measurements were done in a three-electrode experimental setup. Platinum foil with the same area of the working electrode and Hg/HgO electrodes was used as the counter and reference electrodes, respectively. All the electrochemical measurements were carried out in 2 mol/l KOH electrolyte and using a CHI760B electrochemical workstation (CHI instruments).

Results and discussion

Figure 1 shows the thermogravimetric–differential thermogravimetric (TG–DTG) curves of the MnO_2 obtained by using supramolecular as template, dried at room temperature in air. The first weight loss at 42~100 °C resulted from the removal of physically absorbed water, and the second step weight loss at 100~298 °C was due to the removal of chemically bound water and decomposition of partial polymer in the sample. DTG displayed two exothermic peaks at 190.3 and 460.7 °C. The peak at 190.3 °C is attributed to the removal of chemically bound water and decomposition of partial polymer; the peak at 460.7 °C may be ascribed to the transformation of MnO_2 into Mn_2O_3 as depicted in literature [11].

Figure 2a displays the XRD patterns of MnO_2 obtained by different preparation condition and sintering at 200 °C for 1.5 h. It can be seen clearly that these peaks of MnO_2 prepared using and without using supramolecular as template are broad, which indicate the amorphous nature of the products. However, the peaks' intensity of MnO_2 obtained by using supramolecular as template is dramatically lower than that of the material prepared without using supramolecular as template. It can be explained that the presence of supramolecular is favorable in forming amorphous structure of materials. Figure 2b illustrates the XRD patterns of MnO_2 obtained by using supramolecular as template and heat-treated at different temperature. It is clearly seen that all of these peaks for MnO_2, heat-treated at 200 and 300 °C, have an amorphous nature. The XRD patterns of MnO_2 heat-treated at 400 °C correspond to
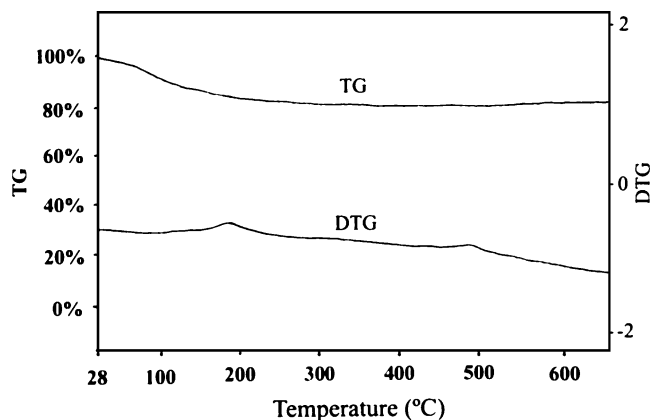

Fig. 1 TG and DTG curves for MnO_2 precursor obtained by using template (heating rate 10 °C/min)
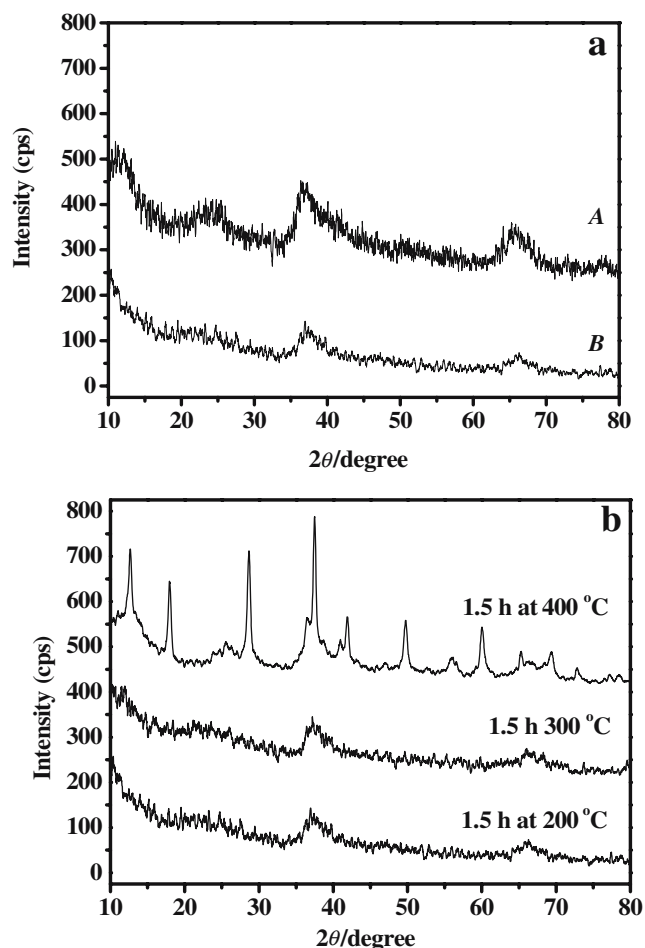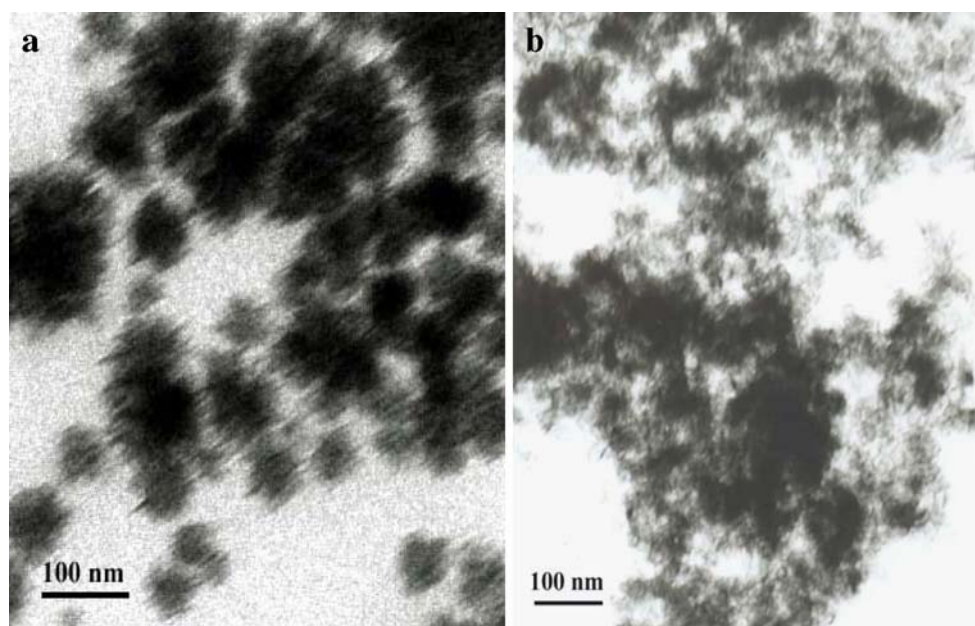
Fig. 2 a XRD patterns of MnO_2 powder prepared at different conditions and sintering at 200 °C for 1.5 h (*A* the MnO_2 obtained without using supramolecular template; *B* the MnO_2 obtained by using supramolecular template). **b** XRD patterns of MnO_2 powder prepared using supramolecular template and sintering at different temperature

crystalline α-MnO_2. The result is in accordance with the standard spectrum (Joint Committee for Powder Diffraction Studies, card no. 44-0141).

The morphology of the samples prepared under different conditions was observed by TEM. Figure 3a presents the morphology of the MnO_2 powders obtained at 200 °C for 1.5 h without using supramolecular as template. It can be clearly seen that the sample was actually made up of small lamellar nanoparticles that agglomerate with each other to form the clusters. Figure 3b displays the morphology of MnO_2 obtained at 200 °C for 1.5 h and using supramolecular as template. The MnO_2 is very loose and consisted of many small particles. Comparing the morphology of MnO_2 obtained under different conditions, great distinctions could be clearly seen, which indicates that the supramolecular template (PAM and PVA) has played an important role in controlling the morphology of samples.

To further analyze the structure of the MnO_2 obtained at different conditions, the nitrogen adsorption–desorption isotherms were measured. The BET surface areas, calculated from adsorption isotherms, show that the surface area of the MnO_2 obtained using supramolecular template is 171 m^2/g, which increases significantly compared with that of the MnO_2 prepared without using supramolecular template (85 m^2/g). Figure 4 is the adsorption/desorption isotherm of the samples obtained using supramolecular template. It shows a strong hysteresis loop, which is an adsorption–desorption characteristic of the porous materials. This means that PAM and PVA are very helpful to control and maintain the mesopore structure. In the process of redox reaction, the supramolecular provides a fixed template for the formation of mesoporous amorphous MnO_2, which contributes to the stable skeleton of the

Fig. 3 TEM of MnO_2 obtained at 200 °C by different preparation conditions. (**a** MnO_2 obtained without using supramolecular template, **b** using supramolecular template)

Fig. 4 N$_2$ gas adsorption–desorption isotherm (**a**) and pore size distributions (**b**) of MnO$_2$ obtained at 200 °C
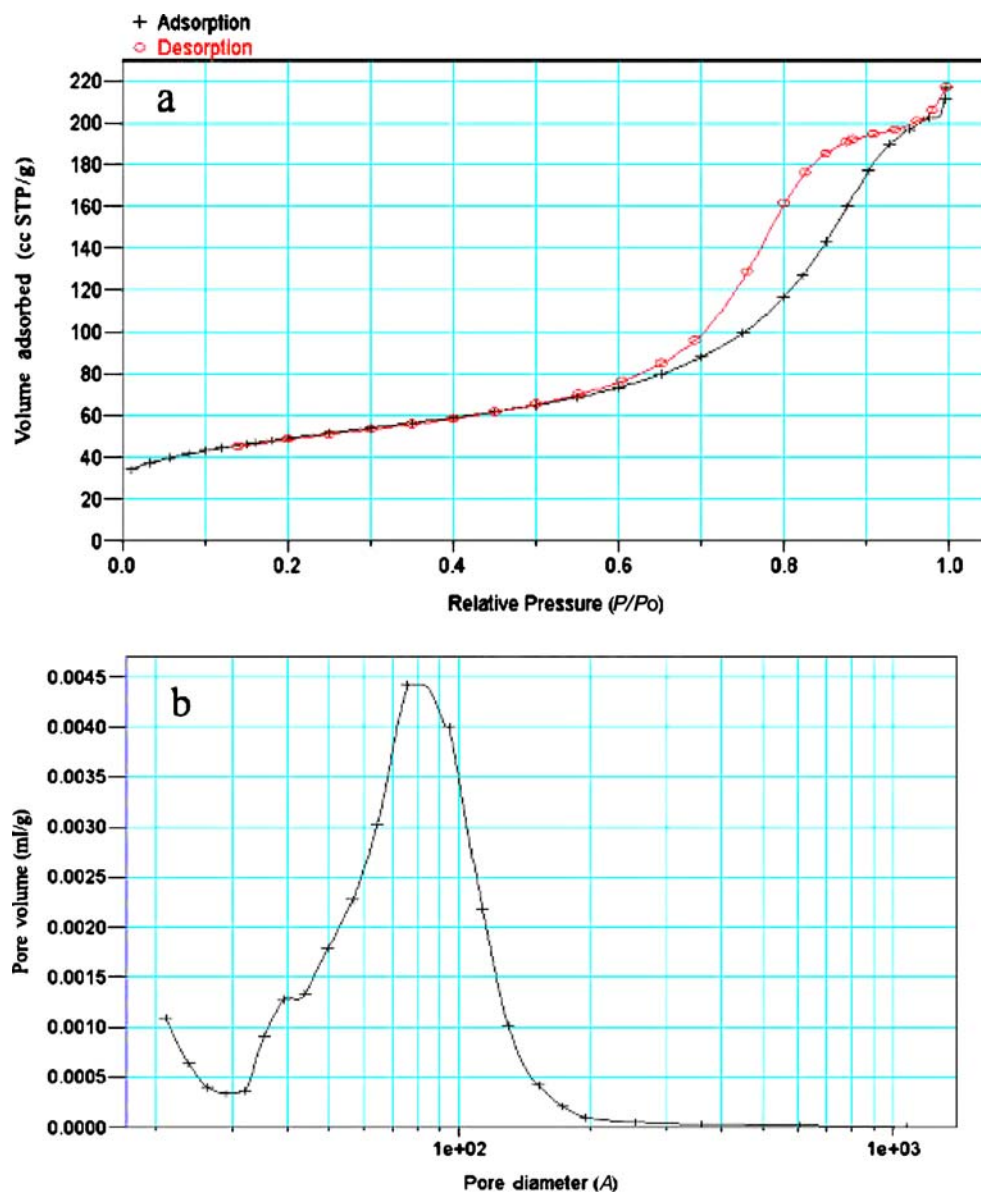
mesoporous MnO$_2$. After calcination at 200 °C for 1.5 h, some supramolecular template residue and chemically bound water are removed from the pore system, but the pore skeleton of the sample is well sustained.

From the above results, it can be seen clearly that the MnO$_2$ prepared by using supramolecular as template is a more potential candidate, which can be applied in a supercapacitor.

To evaluate the microstructure of as-synthesized materials and their electrochemical property, these samples are fabricated to electrodes of supercapacitors and characterized with cyclic voltammograms (CV) and chronopotentiometric measurements.

Typical CV for MnO$_2$ heat-treated at 200 °C using and without using supramolecular as template are shown in Fig. 5. The potential varies between −0.15 and 0.45 V vs

Hg/HgO reference electrode at sweep rates of 5, 10, and 20 mV/s. As can be seen from Fig. 5a and b, the curves of the two samples show no peaks, which indicate that the electrode is charged and discharged at a pseudoconstant rate over the complete voltammetric cycle, as solution resistance can distort current response at the switching potential, and this distortion is dependent upon the scan rate [12]. At low scan rates (5 mV/s), the MnO$_2$ shows almost ideal capacitive behavior. However, with the scan rate increasing, the deviation from rectangularity of the CV becomes obvious. Comparing Fig. 5a with b, at same scan sweep, the current of the sample obtained without using supramolecular as template is dramatically lower than that of the sample prepared using supramolecular as template. These results are in agreement with that of TEM and BET analyses and further confirmed that the MnO$_2$ obtained
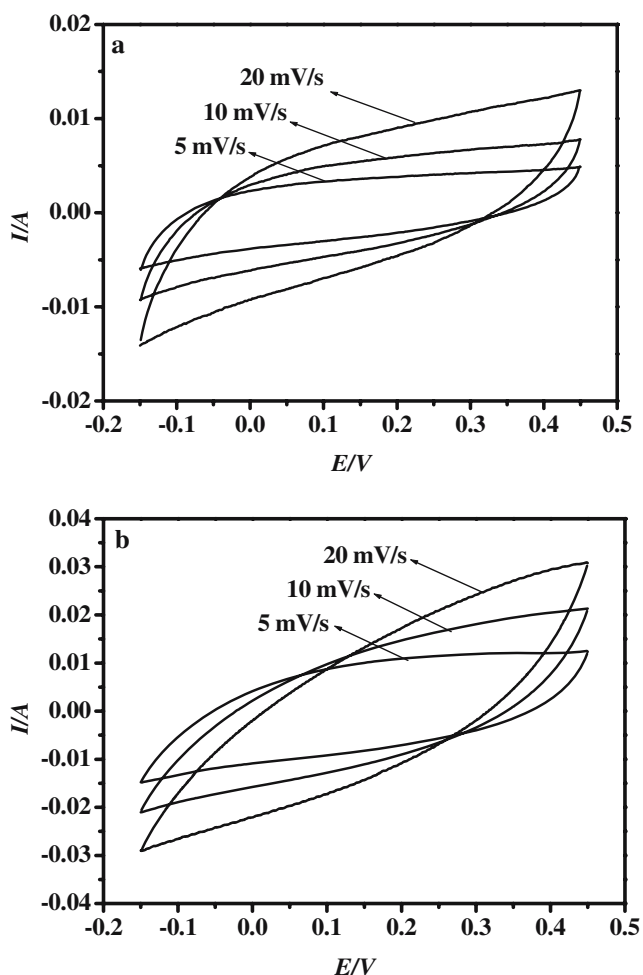
Fig. 6 Charge/discharge curves of MnO_2 formed at 200 °C in the potential rage from −0.15 to 0.45 V at different current densities

Fig. 5 CV curves of MnO_2 heat-treated at 200 °C at different scan rates. (a MnO_2 obtained without using supramolecular template, b using supramolecular template)

the active materials is examined by chronopotentiometry. The specific capacitance can be obtained from Eq. (1)

$$C = \frac{I}{[(dV/dt) \times w]} \tag{1}$$

Where I (mA) and dV/dt (mV/s), respectively, denote the applied galvanostatic current and the slope of chronopotentiometric curve when the curve is approximately linear and symmetric (this can be confirmed by Fig. 6); W (g) represents the mass of electroactive material. Therefore, the specific capacitances of MnO_2 heat-treated at different temperatures obtained on the basis of Eq. (1) are shown in Fig. 7.

The MnO_2 obtained at 200 °C yields the highest specific capacitance (about 298.7 F/g), whereas MnO_2 heat-treated at 300 °C shows a correspondingly low specific capacitance of 258 F/g, and annealing at 400 °C, it exhibits a very low specific capacitance of 142 F/g. This variation cannot only be explained based on the change of double layer

using supramolecular as template is a good candidate for supercapacitor electrode material. Hence, further study was focused on the MnO_2 obtained using supramolecular as template.

Figure 6 shows the charging and discharging behavior of the synthesized MnO_2 powder formed at 200 °C using supramolecular as template. The typical results are measured from −0.15 to 0.45 V in 2 mol/l KOH at different current density (2.5, 5 and 10 mA). As shown in Fig. 6, the charge curves are very symmetric to their corresponding discharge counterparts in the whole potential region, and the slope of every curve is potential–independence and maintains a constant value at a specified current. The results indicate that the mesoporous amorphous MnO_2 powder heat-treated at 200 °C has the ideal capacitive behavior for electrochemical capacitors.

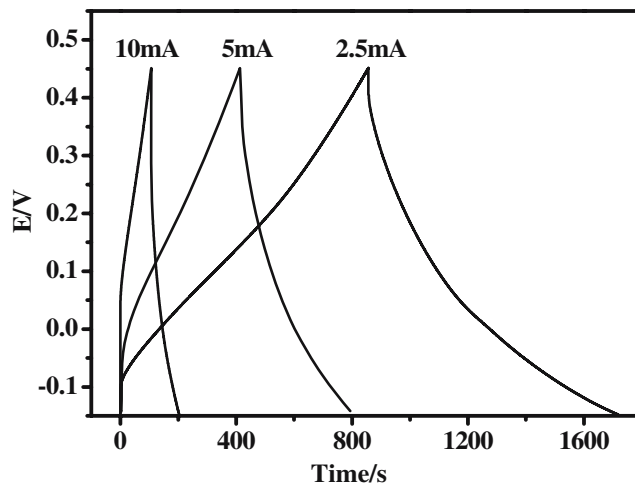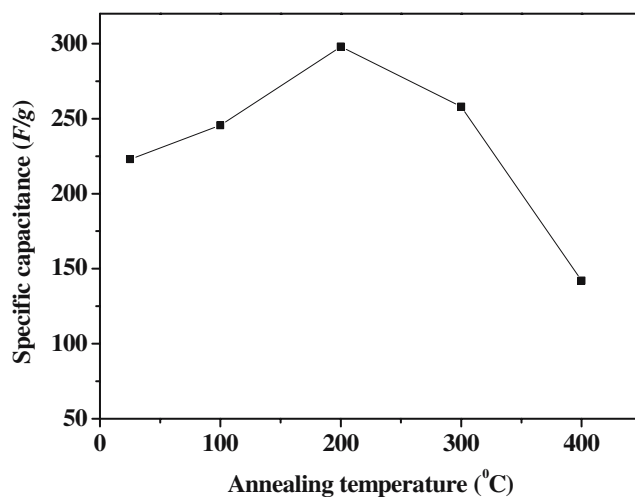To investigate the effect caused by temperature on the capacitance of the samples, the capacitive performance of
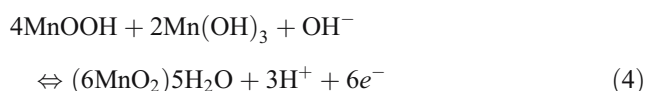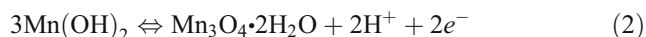

Fig. 7 Electrode-specific capacitance of MnO_2 heat-treated at different temperatures

capacitance, which resulted from the change of surface area, as the material still remained amorphous with larger surface area till 300 °C (listed in Table 1). Although some double layer charging can significantly contribute to the measured capacitance due to the high surface area of this material, it cannot solely explain the whole capacitance of the electrode. The calculation of the pure double layer capacitance using the BET surface area (171 m^2/g for the sample obtained by heating at 200 °C) by using an average value of 20 μF/cm^2 gives a specific capacitance of 34 F/g, which is nine times lower than that measured in this study (298.7 F/g). So it is believed that the main part of the capacitance comes from the pseudocapacitive surface redox process. When the specific surface area of MnO$_2$ electrode material increases, not only the double layer capacitance will increase, the redox active sites will increase subsequently, so the pseudocapacitance will increase significantly.

Chemically bound water is essential for the transportation of active ionic species, so pseudocapacitance of oxide material depends on the water content [13, 14]. Therefore, the crystalline water content is another factor that may be playing an important role. In DTG studies, it can be observed that the complete loss of water content occurs at 289 °C. MnO$_2$ formed at 500 °C is left with no water content leading to the loss of pseudocapacitance.

Furthermore, in an alkaline medium, the electrochemical reactions occurring in MnO$_2$ have been hypothesized as follows [12, 15].

$$3Mn(OH)_2 \Leftrightarrow Mn_3O_4 \cdot 2H_2O + 2H^+ + 2e^- \qquad (2)$$

$$Mn_3O_4 \cdot 2H_2O + OH^- \Leftrightarrow MnOOH + Mn(OH)_3 + e^- \qquad (3)$$

$$4MnOOH + 2Mn(OH)_3 + OH^-$$
$$\Leftrightarrow (6MnO_2)5H_2O + 3H^+ + 6e^- \qquad (4)$$

The charge storage process may be completed by the combination of chemsorption/desorption of ions from the electrolyte and proton insertion from water. The amorphous nature of MnO$_2$ heat-treated at 200 °C is thought to be beneficial to ionic charge transport. Hence, a high specific capacitance is obtained in this study.

Table 1 The BET (N$_2$) specific surface area and average pore size of samples

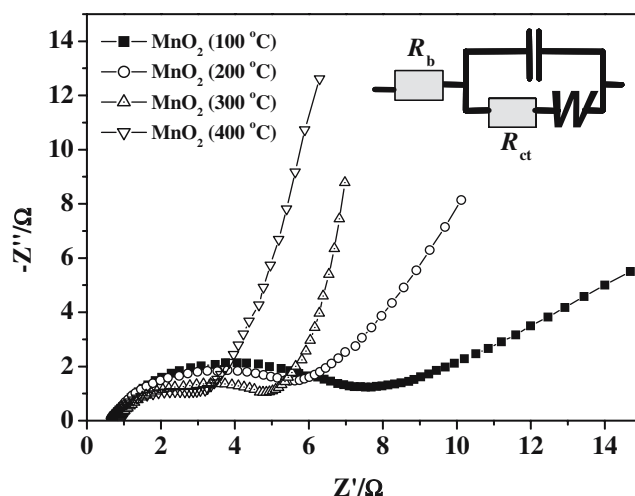| Samples (°C)	Specific surface area (m^2/g)	Average pore diameter (nm)
MnO$_2$ (100)	214	4.8
MnO$_2$ (200)	171	7.8
MnO$_2$ (300)	103	11
MnO$_2$ (400)	87	18

Fig. 8 Complex plane impedance plots of the MnO$_2$ electrode prepared at various annealing temperature at AC voltage amplitude of 5 mV. The *inset* of Fig. 8 is the equivalent circuit

Electrical conduction and ion transfer were investigated by electrochemical impedance spectroscopy (EIS). Figure 8 shows the complex plane plots of the impedance of the MnO$_2$ electrode prepared at various temperatures (at open circuit potential). The EIS of the MnO$_2$ electrode is composed of partially overlapped semicircles and a straight sloping line. Such a pattern of the EIS can be fitted by an equivalent circuit shown in inset of Fig. 8. The R_b is bulk resistance of the electrochemical system, which reflects electric conductivity of the electrolyte and electrodes; R_{ct} is faradic charge–transfer resistance; W is the Warburg impedance related to a combination of the diffusion effects of ion on the interface between the active material particles and electrolyte, which is generally indicated by a straight
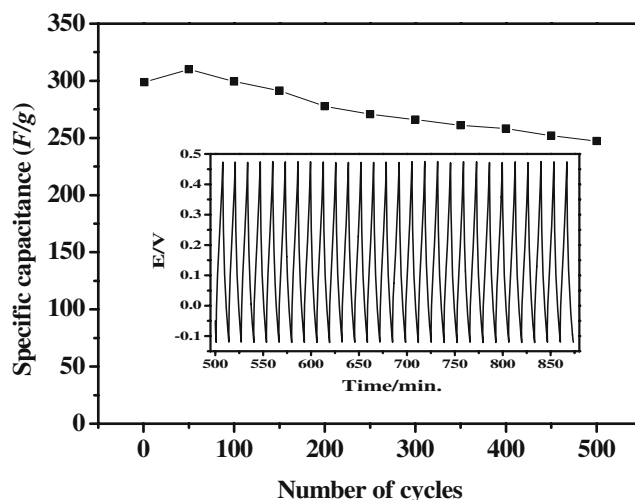

Fig. 9 Cycle-life of the MnO$_2$ electrode at 5 mA in 2 mol/l KOH electrolyte, the *inset* is charge/discharge curves of this electrode

sloping line at low frequency end. The combination of R_{ct} and W is called faradic impedance, which reflects kinetics of the electrochemical reactions [16, 17].

It is clear that the R_{ct} decreased with the increasing of annealing treatment temperature. This can be explained as follows: In MnO_2 (100 °C) electrode that was subjected to the lowest heat treatment temperature, the residual supramolecular in the sample, a nonconductor, can decrease the exchange rate of electrode material and electrolyte ions. As the annealing temperature increased, the supramolecular was oxidized and decomposed. Therefore, the R_{ct} decreased correspondingly.

Furthermore, the slope of the plot at the low frequency end increased with the sintering temperature increasing, which indicates characteristics of a porous electrode strongly controlled by the diffusive resistivity of the electrolyte within the pores of the electrode material [2]. With the increase in the sintering temperature, the increase in the pore diameter can enhance the diffusivity of electrolyte ions in the electrode material. Therefore, the diffusing lines, especially for the MnO_2 (300 and 400 °C), come closer to an ideal straight line along the imaginary axis (Z'').

The long-term cycling stability of composite electrodes made of on the powder obtained at 200 °C upon cycling is investigated, and the variation of specific capacitance over 500 cycles is depicted in Fig. 9. A little increase in capacitance is observed during the first 50 cycles, and thereafter, the capacitance begins to decrease. After 500 cycles, the capacitance is still of the first cycle approximately 83.2%. This demonstrates that, within the voltage window −0.15~0.45 V, the charge and discharge processes do not seem to induce significant structural or microstructural changes of the MnO_2 electrode material as expected for pseudocapacitance reactions. The long-term stability implies that the MnO_2 is a good candidate as a material for a supercapacitor electrode.

Conclusion

Mesoporous amorphous MnO_2 was synthesized by an improved reduction reaction and using supramolecular as template. The amorphous structure was determined by TEM and XRD analysis. The amorphous MnO_2 annealed at 200 °C exhibited the maximum specific capacitance of 298.7 F/g in a 2 mol/l KOH electrolyte at 5 mA. The prepared mesoporous amorphous MnO_2 showed ideal capacitive nature, high specific capacitance, and long cycle life, so it is suitable to be used as electrode material for electrochemical capacitors.

References

1. Srinivasan V, Weinder JW (2000) J Electrochem Soc 147:880
2. Lin C, Ritter JA, Popov BN (1998) J Electrochem Soc 145:4097
3. Hu CC, Tsou TW (2003) J Power Sources 115:179
4. Wu MQ, Snook GA, Chen GZ, Fray DJ (2004) Electrochem Commun 6:499
5. Reddy RN, Reddy RG (2003) J Power Sources 124:330
6. Long JW, Young AL, Rolison DR (2003) J Electrochem Soc 150:A1161
7. Moore TE, Ellis M, Selwood PW (1950) J Am Chem Soc 72:856
8. Pang SC, Anderson MA, Chapman TW (2000) J Electrochem Soc 147:444
9. WangYQ, Yin LX, Palchik O, Hacohen YR, Koitypin Y, Gedanken A (2001) Langmuir 17:4131
10. Lee B, Lu D, Kondo JN, Domen K (2002) J Am Chem Soc 124:11256
11. Reddy RN, Reddy RG (2004) J Power Sources 132:315
12. Jiang JH, Kucernak A (2002) Electrochim Acta 47:2381
13. Takahashi T (1981) Electrochim Acta 26:1467
14. Kim H, Popov BN (2003) J Electrochem Soc 150:D56
15. Messaoudi B, Joiret S, Keddam M, Takenouti H (2001) Electrochim Acta 46:2487
16. Zhang SS, Xu K, Jow TR (2004) Electrochim Acta 49:1057
17. Bao SJ, Liang YY, Zhou WJ, He BL, Li HL (2006) J Power Sources 154:239